Hysteresis Properties of Hexagonal Arrays of FePd Nanowires

María S. Viqueira[1], Sebastián E. García[2], Silvia E. Urreta[1], Gabriela Pozo López[1,2], and Luis M. Fabietti[1,2]

[1]Facultad de Matemática, Astronomía y Física, Universidad Nacional de Córdoba, Argentina
[2]Instituto de Física Enrique Gaviola. CONICET

FePd nanowires (NWs) with different compositions have been grown into anodized aluminum oxide templates (AAO) by AC electrodeposition at room temperature. The effects of nanowire composition and morphology on the hysteresis properties of the ordered array of NWs are investigated. All the NWs are polycrystalline; the Fe-rich wires have a bcc structure while the Pd rich ones are fcc. FePd NWs are ferromagnetic and the spontaneous magnetization is found to be parallel to the nanowire long axis (out of plane easy axis) and both, the saturation polarization and the coercive field increase with the iron content.

***Index Terms*—Alumina template, FePd nanowires, hysteresis properties, shape anisotropy.**

I. Introduction

IRON–PALLADIUM alloys are considered for applications in sensors and microactuators, in hydrogen separation and membrane hydrogenation reactions and also in environmental remediation [1]–[4]. Bulk FePd alloys also exhibit magnetic shape memory (MSM) effect, arising in a reversible thermoelastic martensitic phase transition, induced by either varying temperature or the applied magnetic field [5]. The $\mathrm{L1_0}$-ordered ferromagnetic phase in the FePd system has an anisotropy energy density near $K_u = 18\times10^5\ \mathrm{J/m^3}$, larger than the observed in hcp-Co [6].

These excellent properties of the bulk alloy are not always retained when very small or low dimensional structures are produced, like nanoparticles, nanowires, or thin films. For example, a reduction of the long range order parameter of the $\mathrm{L1_0}$-structure is found in small ($<$5 nm) particles with the consequent loose of the hard magnetic properties [6]; in the same sense, no martensitic phase transformation from fcc Fe–Pd phase to fct FePd phase could be observed in 20 nm diameter nanowire arrays [7], [10]. In this latter case, however, is not clear if it is due to a size effect or to the constraint imposed by the aluminum oxide templates (AAO) template pores.

Ordered arrays of FePd nanowires have been already produced by hard template assisted electrodeposition, using both DC [8] and alternating AC [7], [10] voltages; however highly stable plating baths leading to appropriate deposition conditions to fill the template without surface deposits is rather complex [9].

It has been reported [7], [10] that nanowires with Fe contents lower than 46% have a fcc structure in the as-deposited state; when Fe content is up to 60 at.%, α-Fe, and fcc Fe–Pd phases may coexist in the as-deposited condition. Then, wire composition, length, and diameter are the key parameters determining the magnetic properties.

In this paper, we describe the structure and the room temperature magnetic hysteresis properties of highly ordered FePd nanowire arrays in the as deposited condition; samples were obtained by AC electrochemical deposition into the cylindrical pores of AAO membranes. The collective magnetic behaviors of as deposited nanowire arrays, with different compositions and diameters are characterized.

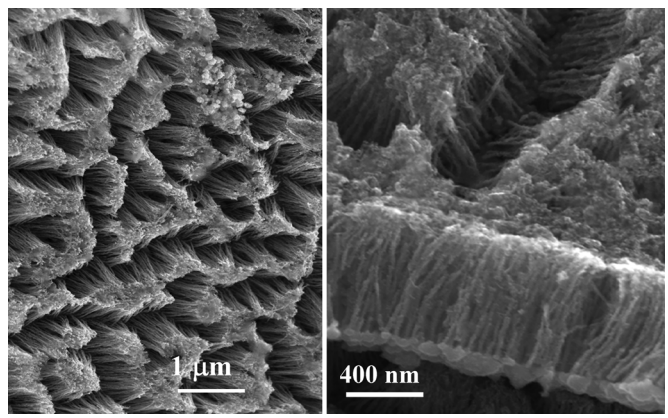

Fig. 1. SEM micrographs showing the $\mathrm{Fe_{50}Pd_{50}}$ nanowires (20 nm in diameter and 0.8 μm in length) after partial dissolution of the alumina template.

II. Experimental Procedure

FePd nanowires with different diameters and compositions were prepared by electrodepositing the metal ions within the pores of AAO; these membranes act as hard templates with a hexagonal array of pores quite uniform in diameter and in length. Porous AAO templates with diameters between 20 and 70 nm and uniform length of about 1 μm were prepared, by a two-step anodizing process on high purity (99.995%) aluminum foils in a 0.3 M oxalic acid solution at 3 °C, by varying DC voltage between 20 and 40 V [11]. Previous to the anodization process the foil was degreased and electropolished. Some templates were further immersed in 0.3 M $\mathrm{H_3PO_4}$ for several minutes to enlarge the diameter and also to reduce the barrier layer thickness [12].

The electrodeposition of FePd nanowire arrays with different compositions was carried out by first preparing different aqueous electrolytic baths containing variable relations of $\mathrm{Fe^{+2}}$ and $\mathrm{Pd^{+2}}$ ions from $\mathrm{FeCl_2}$, $\mathrm{PdCl_2}$, and 30 g/l of $\mathrm{H_3BO_4}$, included to enhance conductivity. The pH value was adjusted to 5 by adding few drops of dilute HCl. Then the electrodeposition of FePd was conducted at room temperature under a sinusoidal wave of 200 Hz and 20 V rms, during a few minutes;

Manuscript received February 16, 2013; revised March 21, 2013; accepted April 09, 2013. Date of current version July 23, 2013. Corresponding author: S. E. Urreta (e-mail: urreta@famaf.unc.edu.ar).

Color versions of one or more of the figures in this paper are available online at http://ieeexplore.ieee.org.

Digital Object Identifier 10.1109/TMAG.2013.2258461

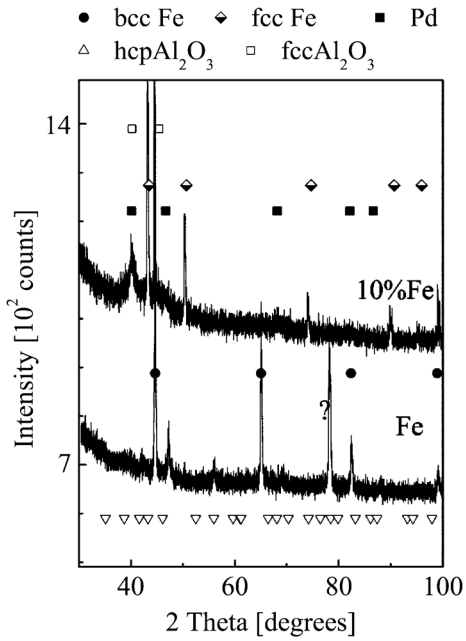

Fig. 2. XRD data corresponding to 26 nm diameter Fe and Pd(Fe) nanowire, after removal of the Al support. The large peak marked by ? could not be properly indexed.

a two electrode electrochemical cell was used, where the AAO template served as a working electrode and a graphite rod as an auxiliary one. The morphology and microstructure of the resulting samples were investigated by scanning electron microscopy (SEM) in a FE SEM Zeiss device, and by X-ray diffraction techniques in a Philips PW 3830 X-ray diffractometer with Cu Kα ($\lambda = 1.5418$ Å), in the 2 θ range between 30° and 90° in the Bragg-Brentano configuration. Samples for XRD measurements were prepared by dissolving the remaining Al substrate in a $CuSO_4$ and HCl solution, while for SEM observation the nanowires were further liberated from the template by dissolving the alumina membrane with aqueous 1 M Na (OH).

To characterize the magnetic properties the hysteresis loops were measured at two different relative orientations between the sample and the applied magnetic field: $\theta = 0°$ (PA, with the magnetic field parallel to the long nanowire axis) and $\theta = 90°$ (PE, with the magnetic field perpendicular to the long nanowire axis). The total magnetic moment of the assembly has contributions from the Al support (paramagnetic), the alumina template (diamagnetic), and the metallic wires filling the pores (ferromagnetic). The measurements were realized in Lakeshore 7300 vibrating simple magnetometer (VSM).

III. Results and Discussion

Fig. 1 shows SEM top and lateral views of $Fe_{50}Pd_{50}$ nanowires after the partial dissolution of the alumina template; the 1 μm length pores were in general not completely filled (mean length about 0.8 μm) but only few surface deposits were observed. Fig. 2 shows the XRD data of pure Fe and $Fe_{10}Pd_{90}$ nanowires after removal of the Al support; these results agree with previously reported data [7]–[10], in the sense that the Pd-rich wires have a fcc Pd(Fe) structure, while Fe-rich ones exhibit a bcc Fe(Pd) phase. In our Pd-rich samples some lines

TABLE I
Parameters From XRD Data

Sample	a_0 [Å]	d [nm]	e x 10^{-3}
Fe	2.877	40±20	3±1
$Fe_{10}Pd_{90}$	3.889	10±2	5±1

Lattice constant a_0, mean crystallite size d, and mean residual stress e in the matrix determined from XRD data in Fig. 2

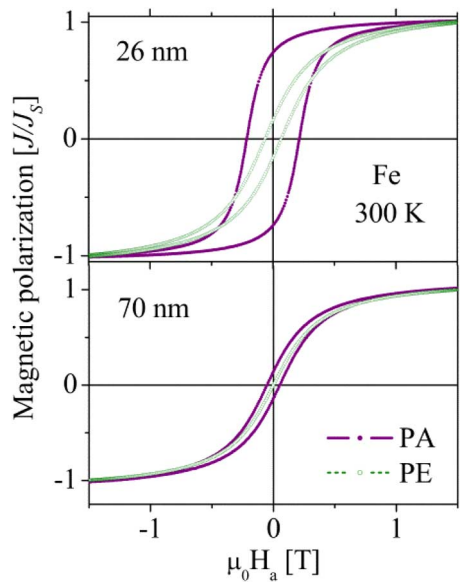

Fig. 3. Room temperature hysteresis loops of Fe nanowires with diameters of 26 and 70 nm and 0.8 μm long. Shape effects are small in the array with the largest diameter.

corresponding to γ-Fe are also found. As expected, no traces of $L1_0$ superstructure peaks are detected in these as deposited samples. The corresponding values of the lattice constant, the mean crystallite size and the mean residual stress measured in samples of Fig. 2 are listed in Table I.

The room temperature hysteresis loops of two arrays of iron nanowires with different diameters are shown in Fig. 3. The loops measured with the applied field parallel (PA) and perpendicular (PE) to the nanowire length are quite different mainly due to a large shape effect. In fact, for pure Fe the shape anisotropy constant and the corresponding anisotropy fields are

$$k_{\text{shape}} = \frac{1}{2} J_S^2 / \mu_0 \Delta N \cong 9.3 \times 10^5 \text{ J/m}^3 \quad (1)$$

$$\mu_0 H_{\text{shape}} A = J_S \Delta N \cong 1.08 \text{ T} \quad (2)$$

where $\Delta N = (N_\perp - N_\parallel) \cong 0.5$ is the difference between normal and parallel (to the wire length) demagnetizing factors, respectively. Then, this shape contribution to the effective anisotropy is larger than that arising from magnetocrystalline coupling ($\mu_0 H^A_{\text{cryst}} = 50$ mT). In "soft-magnetic" wires an empirical rule is [13] that the coecivity is about one third of the theoretical nucleation field. In these ordered arrays, results also indicate [14] that there is a quite strong dipolar field when the saturating field is applied perpendicular to the wire axis, while the dipolar interaction with all the magnetic moments aligned parallel to the wire axis is very weak, and can be ignored. Then,

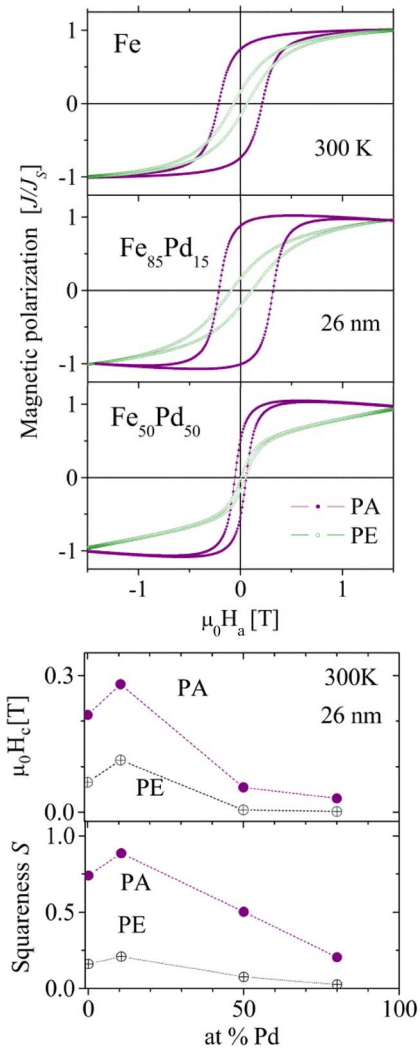

Fig. 4. (a) Room temperature hysteresis loops of 26 nm diameter nanowire arrays with different Pd contents. For all the compositions the samples exhibit an easy axis parallel to the wire length indicating a relatively large shape anisotropy. (b) Room temperature coercivity and squareness measured in 26 nm diameter nanowire arrays with different Pd contents.

the easy magnetization axis becomes determined by the competition of dipolar interactions and the shape anisotropy. It may be observed in Fig. 3 that the arrays have a clear out of plane easy axis (parallel to the wires length) and an in plane hard axis, in both nanowire arrays, 20 nm (aspect ratio $r = 800/20 = 40$) and 70 nm ($r < 10$) in diameter. The relatively high coercivity of these iron nanowire arrays, of about 0.2 T are certainly due to the shape anisotropy. As reported in [7], [10], the coercive field and the loop squareness S ($S = J_R/J_S$, with J_R and J_S the remanent and the saturation polarizations, respectively) are found to decrease when the wire diameter increases.

The effect of the alloy composition is illustrated in Fig. 4; Fig. 4(a) shows the room temperature hysteresis loops of three 26 nm diameter nanowire arrays with different Pd contents; for all the compositions investigated, the samples exhibit an easy axis parallel to the wire length, indicating a relatively large shape anisotropy. It may be also observed—see Fig. 4(b)—that except in the case of the alloy with a small amount of Pd, the loop coercivity and squareness decrease as the Fe content decreases. This can be rationalized by considering that the magnetic polarization of the FePd solid solution is mainly governed by the exchange interaction between Fe atoms; then, decreasing the Fe content in the alloy reduces the saturation magnetization leading to a lower shape anisotropy, and consequently to a smaller coercivity. Assuming that the spontaneous polarization in the alloy can be estimated on the basis of the mixture rule, the shape anisotropy field given by (2) results about 0.9, 0.54, and 0.2 T for compositions $Fe_{85}Pd_{15}$, $Fe_{50}Pd_{50}$, and $Fe_{20}Pd_{80}$, respectively.

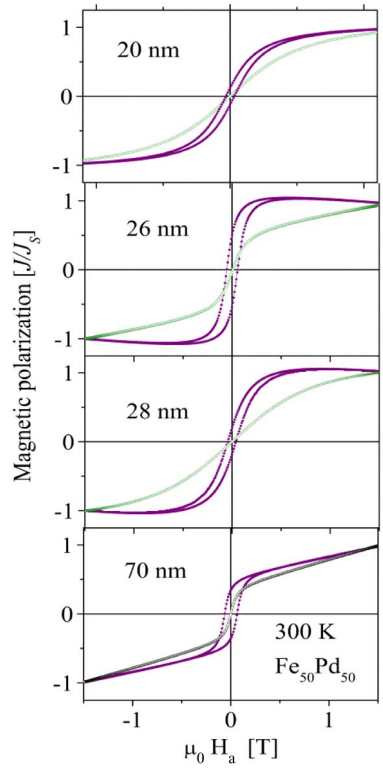

Fig. 5. Room temperature hysteresis loops of $Fe_{50}Pd_{50}$ nanowire arrays with different diameters.

The effect of the nanowire diameter on the hysteresis behavior is more complex and strongly dependent on the wire nanostructure. In single crystalline or large grained nanowires (grain size larger than the domain wall size), the coercive field decreases when the diameter increases because of the onset of nonhomogeneous magnetization modes and/or the appearance of domain walls leading to smaller critical reversion fields. In small grained, polycrystalline nanowires, where a magnetization mechanism involving nucleation and expansion of transversal domain walls is likely to operate, larger diameters are often correlated with larger grain sizes leading to higher nucleation fields. In this sense, a definite trend is found in Fe nanowires of about 40 nm grain size (about twice the magnetic domain wall thickness in Fe), with coercivity largely decreasing when the wire diameter increases, while in samples $Fe_{50}Pd_{50}$ with a grain size of about 10 nm no systematic behavior is observed in the diameter size range between 20 and 30 nm.

IV. Conclusion

Ordered Fe–Pd nanowire arrays with different wire diameters and compositions have been successfully fabricated by AC electrodeposition techniques, using AAO as templates.

For large Fe contents samples are bcc Fe(Pd) alloys while the Pd-rich ones the major phase is fcc Pd(Fe) structure with some crystals of γ-Fe.

The arrays are ferromagnetic in the entire composition range: they have an easy magnetization axis parallel to the wire length (out of the array plane), indicating a relatively large shape anisotropy.

The addition of small amounts of Pd ($\leq$10 at.%) to the iron lattice increases both the loop coercivity and squareness. However, for larger Pd concentrations, these hysteresis parameters both gradually decrease.

ACKNOWLEDGMENT

The authors thank SECyT-UNC, FONCyT, and CONICET for the financial support given to this work.

REFERENCES

[1] D. Vokoun and C. T. Hu, "Two-way shape memory effect in Fe-28.8 at.% Pd melt-spun ribbons," *Scripta Mater.*, vol. 47, p. 453, 2002.

[2] K. J. Bryden and J. Y. Ying, "Nanostructured palladium-iron membranes for hydrogen separation and membrane hydrogenation reactions," *J. Membrane Sci.*, vol. 203, p. 29, 2002.

[3] K. J. Bryden and J. Y. Ying, "Electrodeposition synthesis and hydrogen absorption properties of nanostructured of nanoestructured palladium-iron alloys," *Nanostruct. Mater.*, vol. 9, p. 485, 1997.

[4] B.-Y. Yoo, S. C. Hernadez, B. Yoo, Y. Rheem, and N. V. Myung, "Electrochemically fabricated zero-valent iron, iron-nickel, iron-palladium nanowires for environmental remediation applications," *Water Sci. Technol.*, vol. 55, p. 149, 2007.

[5] H. Uchida, Y. Matsumura, H. Uchida, and H. Kaneko, "Ar ion beam irradiation effects on magnetostrictive characteristics of Tb-Fe thin films," *J. Magn. Magn. Mater.*, vol. 239, p. 540, 2002.

[6] H. Naganuma, K. Sato, and Y. Hirotsu, "Particle size dependence of atomic ordering and magnetic properties of $L1_0$-FePd nanoparticles," *J. Magn. Magn. Mater*, vol. 310, pp. 2356–2358, 2007.

[7] X. L. Fei, S. L. Tang, R. L. Wang, H. L. Su, and Y. W. Du*, Phys. Rev. Lett.*, vol. 68, p. 3745, 1992.

[8] H. Hu, C. Yang, J. Chen, and G. Wu, "Magnetic properties of $Fe_{0.95}Pd_{0.05}$ nanowire arrays," *J. Magn. Magn. Mater.*, vol. 320, pp. 2305–2309, Apr. 2008.

[9] V. Haehnel, S. Fähler, L. Schultz, and H. Schlörb, "Electrodeposition of $Fe_{70}Pd_{30}$ nanowires from a complexed ammonium-sulfosalicylic electrolyte with high stability," *Electrochem. Commun.*, vol. 12, no. 8, pp. 1116–1119, Aug. 2010.

[10] X. L. Fei, S. L. Tang, R. L. Wang, H. L. Su, and Y. W. Du, "Fabrication and magnetic properties of Fe-Pd nanowire arrays," *Solid State Commun.*, vol. 141, pp. 25–28, Oct. 2007.

[11] H. Masuda, "Highly ordered nanohole arrays in anodic porous alumina," in *Ordered Porous Nanostructures and Applications*, R. B. Wehrspohn, Ed. New York: Springer, 2005.

[12] J. W. Diggle, T. C. Downie, and C. W. Goulding, "Anodic oxide films on aluminum," *Chem. Rev.*, vol. 69, no. 3, p. 365, 1969.

[13] R. Skomski, "Exact nucleation modes in arrays of magnetic particles," *J. Appl. Phys.*, vol. 91, pp. 10–15, 2002.

[14] Q.-F. Zhan, J.-H. Gao, Y.-Q. Liang, N.-L. Di, and Z.-H. Cheng, "Dipolar interactions in arrays of iron nanowires studied by Mössbauer spectroscopy," *Phys. Rev. B*, vol. 72, p. 024428, 2005.